Embedded Silicon Nanocrystals Studied by Photoluminescence and Raman Spectroscopies: Exciton and Phonon Confinement Effects

ARTICLE *in* THE JOURNAL OF PHYSICAL CHEMISTRY C · SEPTEMBER 2010

Impact Factor: 4.77 · DOI: 10.1021/jp1044095

7 AUTHORS, INCLUDING:

Patrice Miska
University of Lorraine
74 PUBLICATIONS **467** CITATIONS
SEE PROFILE

Herve Rinnert
University of Lorraine
102 PUBLICATIONS **1,012** CITATIONS
SEE PROFILE

M. Vergnat
University of Lorraine
131 PUBLICATIONS **1,250** CITATIONS
SEE PROFILE

Embedded Silicon Nanocrystals Studied by Photoluminescence and Raman Spectroscopies: Exciton and Phonon Confinement Effects

Patrice Miska,[†] Manuel Dossot,*[,‡] Thi D. Nguyen,[†,‡] Matthias Grün,[†] Hervé Rinnert,[†] Michel Vergnat,[†] and Bernard Humbert[§]

Institut Jean Lamour, UMR 7198 CNRS, Nancy Université, UPV Metz, Faculté des Sciences et Technologies, Bvd des Aiguillettes, B.P. 70239, F-54506 Vandœuvre-lès-Nancy Cedex, France, Laboratoire de Chimie Physique et Microbiologie pour l'Environnement LCPME, UMR 7564 CNRS, Nancy Université 405, rue de Vandoeuvre, F-54600 Villers-lès-Nancy, France, and Institut des Matériaux Jean Rouxel (IMN), UMR 6502 CNRS, Université de Nantes, 2 rue de la Houssinière, B.P. 32229, F-44322 Nantes Cedex 3, France

Received: May 14, 2010; Revised Manuscript Received: August 17, 2010

The optical and vibrational properties of silicon nanocrystals are studied in two systems elaborated by evaporation. The first one is constituted by a thick SiO layers. The second one is a multilayered sample made by successive evaporations of SiO and SiO_2 layers with controlled thicknesses. The luminescence and Raman spectra are fitted by phenomenological exciton and phonon confinement models accounting for the size distribution of the embedded nanocrystals. The coherence between the two models and experimental data is demonstrated and gives support to the notion of exciton and phonon confinement effect in silicon nanocrystals embedded within silica matrix.

Introduction

Silicon nanostructures have attracted much attention since the discovery of a strong visible photoluminescence emitted by porous silicon (Si).[1] The rich potential of Si nanocrystals lies in the fact that their optical properties are quite correlated to their size and morphology. Potential applications concern for instance the development of new optoelectronic devices at the nanometric spatial scale, but there is also a sound theoretical interest for such quantum dots due to spatial confinement of electronic and phononic wave functions. Several important difficulties are commonly encountered to elaborate the Si nanocrystals: (i) the control of the average size of the grains and the dispersion of diameters, (ii) the shape of the grains (spherical or elongated), (iii) the control of surface defects, and (iv) for embedded Si nanocrystals in a solid matrix, the role of this matrix on the residual stress and quantum confinement.

The formation of Si nanocrystals (nc-Si) within a matrix of SiO_2 can be realized following many different techniques such as ion implantation,[2−4] plasma-enhanced chemical vapor deposition,[5] laser pyrolysis of silane in a gas flow reactor,[6] or magnetron sputtering of SiO_x thin film and postdeposition annealing process.[7] To better control the size of the created Si nanocrystals, embedding a SiO layer of thickness e between insulating SiO_2 layers gives the possibility to control average diameter. In such SiO_2/SiO multilayers, the average diameter is narrowly distributed around the value of e.[8−10]

In this study, we analyzed the optical and vibrational properties of nc-Si in two systems elaborated by evaporation in the same experimental conditions. The first one is constituted by a thick SiO layer. The second one is a multilayer sample made by successive evaporations of thin SiO and SiO_2 layers. After annealing, silicon nanocrystals (nc-Si) appear due to the demixion of SiO in Si and SiO_2. The nc-Si are then analyzed by photoluminescence (PL) and Raman spectroscopies. The obtained PL and Raman spectra are modeled by taking into account the spatial confinement of excitons and phonons in nanocrystals with a size distribution and the results are compared to the size distribution obtained by electronic microscopy.

Experimental Methods

Elaboration of Silicon Nanocrystals. The films were deposited by evaporation in an ultra-high vacuum chamber (10^{-7} mbar) on silicon substrates maintained at 100 °C. The deposition rate of 1 Å s^{-1} was controlled by a quartz microbalance system. A 200 nm thick SiO monolayer was obtained by evaporation of SiO powder from a tantalum boat. The sample, called monolayer in the following, was then annealed at temperatures between 300 and 940 °C in order to induce the phase separation of SiO to form Si nanostructures and SiO_2. The SiO/SiO_2 multilayer was obtained by successive evaporations of SiO and SiO_2 from the thermal source and an electron beam gun, respectively. The SiO_2 barrier thickness was fixed at 5 nm and the thickness of SiO active layers was equal to 4.5 nm (by taking into account the uncertainty of the measure of the thickness during the deposition process). The final SiO/SiO_2 doublet number is 22 and the total film thickness was equal to 200 nm. The chemical composition of the layers versus the annealing temperature was checked by FTIR spectroscopy. The corresponding spectra are reported in Figure S1 of the Supporting Information and confirm the demixion process of the SiO layer in SiO_2 and Si. The multilayered samples were then annealed at 850 and 1050 °C. The total annealing process duration was around 25 min under vacuum (10^{-6} Torr) and the samples were cooled 5 min after reaching the annealing temperature. For these multilayer samples, the presence of a SiO_2 thermal barrier limited the diffusion of atoms. It yielded the formation of nc-Si with sizes limited by the thickness of the initial SiO layer.[9,10] Figure S2 of the Supporting Information shows an example of

* To whom correspondence should be addressed. E-mail: manuel.dossot@lcpme.cnrs-nancy.fr.
[†] Institut Jean Lamour, UMR 7198 CNRS.
[‡] Laboratoire de Chimie Physique et Microbiologie pour l'Environnement LCPME, UMR 7564 CNRS.
[§] Institut des Matériaux Jean Rouxel (IMN), UMR 6502 CNRS.

10.1021/jp1044095
Published on Web 09/27/2010

an HR-TEM image of a unique silicon nanocrystal. The difference between the two ranges of annealing temperature for mono- and multilayer samples comes from the fact that the temperature of the demixion process is lower in the case of the monolayer sample. Indeed, the very low thickness of the SiO layers in the multilayer samples yields a delay in the demixion process and requires a higher temperature to observe the crystallization of nc-Si. If higher temperatures are used for the monolayer samples, the samples are destroyed.

Luminescence Experiments. PL measurements were performed with a monochromator equipped with a 150 grooves/mm grating and a charge-coupled device detector cooled at 140 K. The excitation wavelength was 313 nm obtained by a mercury arc lamp source and proper optical filter. The response of the detection system was precisely calibrated with a tungsten wire calibration source. For PL measurements at low temperature, the sample was cooled by a flux of cooling nitrogen. The temperature regulation was ±0.1 K.

Raman Scattering Experiments. Raman scattering spectra were acquired on a spectrometer equipped with a liquid N_2 cooled CCD detector. The laser wavelength was the 488 nm emission line of an Ar^+ laser. A confocal microscope was used and the laser was focused on the sample by a ×50 objective (numerical aperture of 0.55). The laser irradiance was kept low (<1 kW cm^{-2}) to avoid any heating effect. This was verified by checking the phonon mode at 522.5 cm^{-1} of the bulk silicon substrate after a quite long period of laser irradiation (1 h). Note that the absolute position of the bulk silicon phonon mode depends on the absolute calibration of the spectrometer and the temperature of the sample. It is common to use the emission line of mercury (from neon lamp) to perform a calibration of the spectrometer in absolute wavenumbers. However, using a blue laser at 488 nm, the spectral position of the mercury line and the spectral position of the phonon mode of bulk silicon are greater than the range of wavenumbers authorized by the high resolution grating at 1800 gr/mm. Therefore, it is necessary to move the grating after absolute calibration to retrieve the silicon spectrum, which always induces a wavenumber shift of 0.1−0.3 cm^{-1}. We thus have chosen to calibrate the relative wavenumber by imposing the bulk silicon mode at 522.5 cm^{-1} for the non-annealed sample to avoid any spectral drift. The entrance slit of the spectrometer was fixed at 40 μm to obtain the best spectral resolution, i.e. 1.2 cm^{-1}. This enabled us to measure the spectral full width at half-maximum (fwhm) of the bulk silicon phonon at 522.5 cm^{-1} at 300 K, which was 3 cm^{-1}. The samples were analyzed at several locations and the results were always consistent for a given sample. It is interesting to note that the laser line at 488 nm enabled us to record a resonant Raman spectrum for nc-Si, whereas the 514 nm laser line available on the argon laser only revealed the phonon modes of the silicon substrate. This fact agrees with a higher band gap of nc-Si compared to bulk Si (see below).

Results

The 200 nm Monolayer Sample. Photoluminescence spectra of the monolayer samples annealed at different annealing temperatures T_a are reported in Figure 1a. For T_a below 600 °C, the photoluminescence band, visible at around 540 nm (2,3 eV), has been attributed to pure SiO[10] and may correspond to the luminescence of the defects in this material. For higher temperatures, this band disappears and a new band appears at higher wavelengths. With annealing, this band shifts toward higher wavelength and considerably broadens. In this system, the demixion process yields the formation of amorphous silicon nanoclusters via diffusion of silicon atoms, contrary to sputtered SiO_x films.[7] Therefore in the absence of any thermal diffusion barrier, large silicon structures are formed by diffusion and coalescence of silicon atoms. Then, the higher T_a is, the bigger the aggregates are, and the wider is the size distribution of these particles within the 200 nm thickness of the SiO layer. Consequently, due to coalescence phenomenon, the quantum confinement is less efficient, which explains the decrease and the red shift of the maximum of the luminescence intensity with high-temperature annealing. The photoluminescence disappears before the crystallization of silicon.

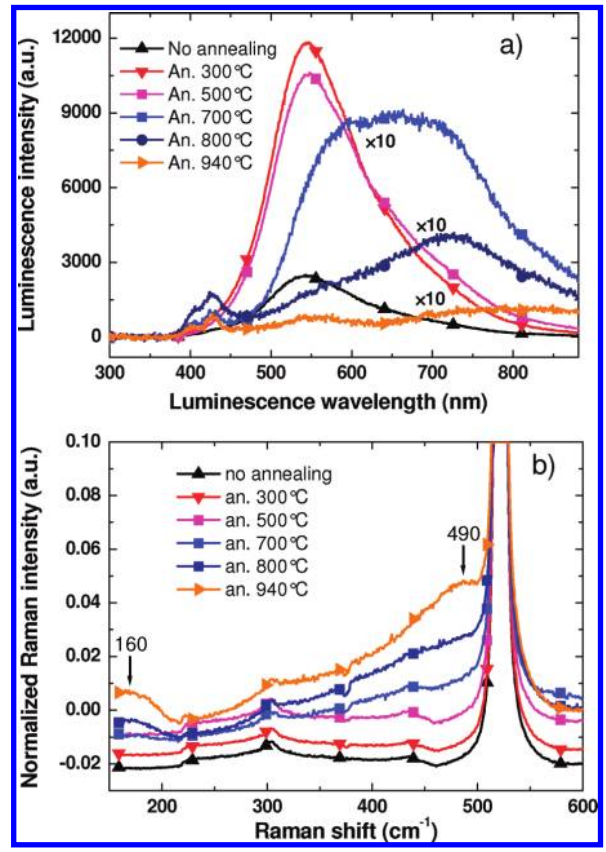

Figure 1. (a) Luminescence spectra of 200 nm thick SiO samples (monolayer) annealed at different temperatures and (b) Raman scattering spectra of the samples annealed at different temperatures.

The corresponding Raman spectra for all these samples are reported in Figure 1b. With increasing T_a, two Raman bands at around 490 and 160 cm^{-1} are growing up, indicating the formation of amorphous silicon within the SiO layer. Figure 2 shows the difference spectrum between the monolayer sample annealed at 940 °C and the as-deposited sample. The structure of the resulting band has been spectrally decomposed by using four Gaussian functions. The band at 479 cm^{-1} is characteristic of the TO phonon modes of amorphous Si clusters, whereas those at 415 and 333 cm^{-1} can be assigned to the LO and LA phonon modes of these amorphous structures. The band at 495.8 cm^{-1} could be attributed to either the D_1 defect band of the SiO_2 phase formed by the demixion process or a TO-LO splitting at the L point of the first Brillouin zone of amorphous silicon clusters. No clear signal for Si nanocrystals is obtained by this spectral subtraction procedure since the annealing temperatures are too low to obtain crystallization or, if the crystallization occurs, the silicon crystals have dimensions much larger than a few nanometers. These experiments show that it is necessary to better control the size of the silicon aggregates until the

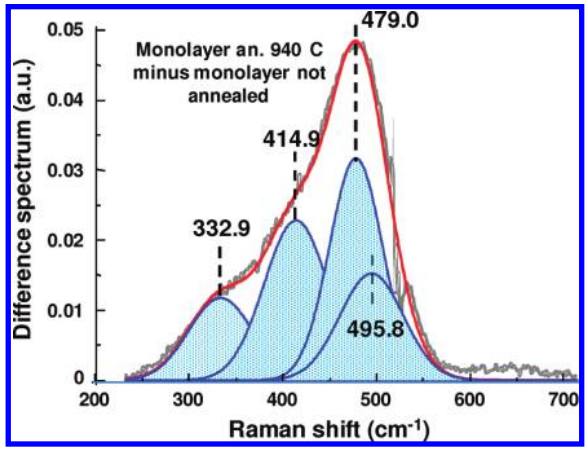

Figure 2. Spectral decomposition by Gaussian functions of the difference spectrum obtained by subtracting the spectrum of the as-deposited monolayer to the spectrum of the monolayer annealed at 940 °C.

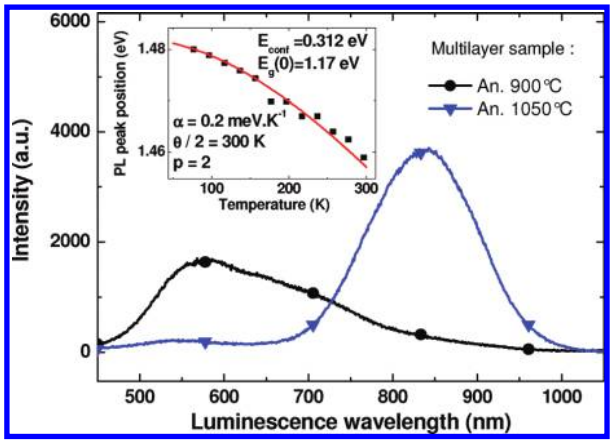

Figure 3. Photoluminescence spectra of the multilayer sample annealed at 900 and 1050 °C. The evolution of the energy of the PL peak position for the sample annealed at 1050 °C is reported in the insert with a fit by the Pässler equation (eq 1).

crystallization, which can be following the strategy of multilayered structures.

Multilayered Samples. Figure 3 reports the photoluminescence spectra of the multilayered samples annealed at two different temperatures T_a. For T_a = 900 °C, no significant phenomenon occurs. A large PL peak, centered at around 570 nm, corresponds to the defects in silica previously observed for the monolayer sample. For T_a = 1050 °C, the luminescence peak at 570 nm is strongly reduced and a large and symmetric peak centered at 848 nm can be observed. These signals can be attributed to the luminescence of silicon nanocrystals[10] and can be the sign of a quantum confinement of excitons in the silicon nanostructures. The verification of the origin of the main PL peaks centered at 848 nm has been done by analyzing the position of the luminescence maximum of the samples with temperature. The insert of Figure 3 reports the energy of this maximum for the multilayered sample versus the analysis temperature. We observe a decrease of the maximum emission energy with an increase of the sample temperature. Pässler et al.[11] have modeled the effect of temperature on the band gap energy of bulk semiconductors, and this equation can be applied to luminescent nanocrystals by using eq 1:

$$E_g(T) = E_{conf} + E_g(0) - \frac{\alpha\Theta}{2}\left[\sqrt[p]{1 + \left(\frac{2T}{\Theta}\right)^p} - 1\right] \quad (1)$$

In this equation, $E_g(0)$ is the gap energy of bulk silicon at 0 K (1.17 eV), E_{conf} is the confinement energy in eV, α is a parameter that represents the slope of the curve at $T \rightarrow +\infty$, Θ ($= \hbar\omega/k$) is related to the average phonon temperature in the material, and p is an exponent parameter (between 2 and 3). The experimental data in the insert of Figure 5 for T_a = 1050 °C have been successfully fitted by this equation. The corresponding values of E_{conf}, α, Θ/2, and p are also reported in the inset of Figure 3. The values found for α, Θ/2, and p are close to the ones reported in the literature for bulk silicon[11] and the confinement energy is found to be significant at ∼0.3 eV. This magnitude of the confinement energy and the fact that the energy of the maximum PL peak of the multilayer samples can be modeled by eq 1 both confirm the presence of nc-Si in the samples. We can say that the main PL peak at around 848 nm originates from exciton recombination in nc-Si. The fwhm of the multilayer PL peak, ∼150 nm for the sample annealed at 1050 °C, is smaller than that of the monolayer sample, ∼280 nm for the sample annealed at 900 °C. This observation validates the multilayer approach to obtain both a narrower size distribution of nc-Si and a final structure (matrix + nanocrystals) with fewer defects.

The corresponding Raman scattering spectra of the multilayer samples are reported in the insert of Figure 4. An intense phonon peak around 520 cm^{-1} assigned to the crystalline silicon Raman mode is clearly observed. It corresponds to the superposition of the phonon mode of bulk silicon of the substrates (near 522.5 cm^{-1}) and the phonon modes of nc-Si. A small but significant downshift of the Raman peak can be seen for the samples annealed at 1050 °C in comparison with the Raman peak of the as-deposited sample. Such downshift has been attributed in literature as a sign of the quantum confinement of phonons inside the silicon nanocrystals.[12] The normalized difference spectra between the annealed and the as-deposited samples are also plotted in Figure 4. The difference spectrum of the sample annealed at 1050 °C is downshifted if compared to the bulk silicon since the maxima of this difference spectrum is located around 519 cm^{-1}. The spectrum is nonsymmetric and broadened in the low-wavenumber side, which is a specific feature of phonon confinement in nanostructures that leads to a relaxation of the **q**-vector selection rule.[12] In the following, the multilayer sample annealed at 1050 °C, which clearly contains silicon nanocrystals, will be chosen as a good material to test both exciton and phonon confinement models.

Discussion

Confinement Model for Luminescence and Raman Spectra. Following the approach developed by Meiers et al.,[13] the photoluminescence emission properties of the nc-Si sample were modeled as the sum of individual contributions of particles of diameter ϕ, which was assumed to follow a log-normal distribution law. The PL emission intensity $I_{PL}^{np}(h\nu,\phi)$ of one particle of diameter ϕ is given by a Gaussian function according to eq 2:

$$I_{PL}^{np}(h\nu, \phi) = \frac{1}{\Delta E\sqrt{2\pi}} \exp\left(-\frac{[h\nu - E_g(\phi)]^2}{4\Delta E^2}\right) \quad (2)$$

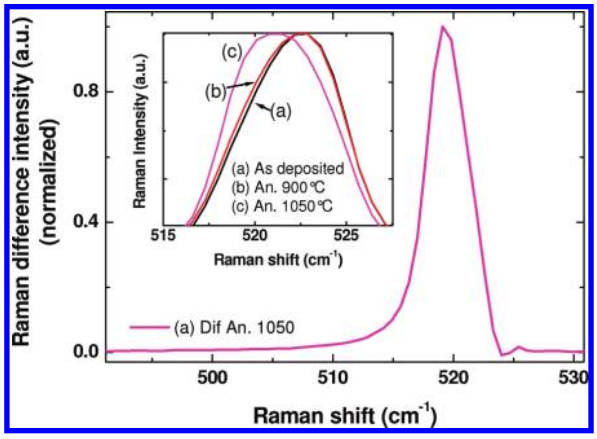

Figure 4. Raman scattering difference spectra of the multilayer samples corresponding to the difference between annealed and non-annealed samples. The original Raman peaks are plotted in the insert as a function of the annealing temperature.

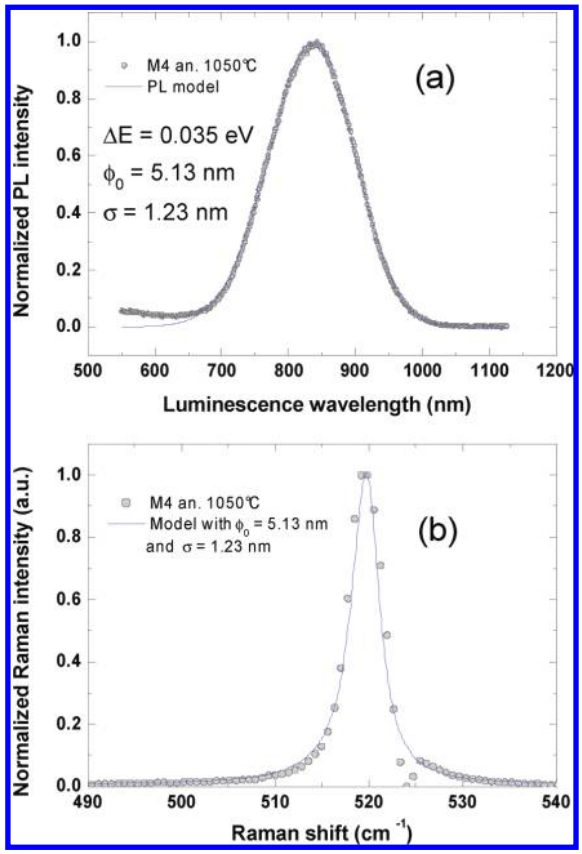

Figure 5. (a) Modeling of the luminescence emission band of the nc-Si of the multilayer sample annealed at 1050 °C using a log-normal statistical law for taking into account the diameter distribution of the nc-Si. ϕ_0 and σ are parameters for the central diameter and the distribution width, respectively. (b) Modeling of the Raman band of the same sample. The experimental spectrum was obtained by subtracting the spectrum of the as-deposited multilayer sample to the one annealed at 1050 °C. The log-normal law for diameter distribution obtained by fitting the luminescence band was applied to the phonon confinement model by using the same values for ϕ_0 and σ.

In this equation, ΔE is the spectral bandwidth of the emission band, ν is the frequency, and $E_g(\phi)$ is the energy band gap for the Si-nc. The later is supposed to follow the experimental relationship eq 3 reported by Delerue et al.:[14]

$$E_g(\phi) = E_0(\text{Si bulk}) + \frac{3.73}{\phi^{1.39}} \quad (3)$$

where E_0 is the indirect band gap of bulk Si (1.17 eV) and ϕ is the nc-Si diameter in nm. The probability to have a nc-Si of diameter ϕ is modeled by using a log-normal distribution law[13] (eq 4):

$$p(\phi, \phi_0, \sigma) = \frac{1}{\sqrt{2\pi}} \frac{1}{\phi \ln(\sigma)} \exp\left(-\frac{1}{2}\left(\frac{\ln(\phi/\phi_0)}{\ln(\sigma)}\right)^2\right) \quad (4)$$

where ϕ_0 is the average diameter and σ is the width of the diameter distribution ($\ln(\sigma)$ being the width of the log-normal distribution). Then, the total photoluminescence spectrum can be given by eq 5:

$$I_{PL}^{tot} = \int_{\phi=0}^{\infty} f_{osc}(\phi) \cdot p(\phi, \phi_0, \sigma) \cdot I_{PL}^{np}(h\nu, \phi)\, d\phi \quad (5)$$

with the oscillator strength given by[13]

$$f_{osc}(\phi) = 1.4 \times 10^{-6} + 1.7 \times 10^{-6} \exp\left(\frac{11.24}{\phi^{1.39}}\right) \quad (6)$$

This model can be adjusted to experimental data by fitting the three parameters ΔE, ϕ_0, and σ.

The Raman scattering spectra were also adjusted by a phenomenological model based on the quantum confinement effect and recently published by Faraci et al.[15] These authors have proposed a new confinement function for modeling the Raman spectrum of a particle with a given diameter ϕ. We have extended this model by including the distribution in diameters of the nc-Si, and using the same log-normal statistical law given in eq 4. In the confinement model, the Raman spectrum is calculated by eq 7 that uses the confinement coefficient $C(\mathbf{q},\phi)$, $\mathbf{q}$ being the reciprocal phonon wave vector that can explore the entire first Brillouin zone of the crystal due to the confinement effect.

$$I_{Raman}(\omega) \propto [n(\omega) + 1] \int_{BZ} C(\mathbf{q}, \phi)^2 L(\omega, \mathbf{q})\, d^3\mathbf{q} \quad (7)$$

Here, ω is the Raman wavenumber, $n(\omega) + 1$ is the statistical Bose−Einstein factor for phonons, $C(\mathbf{q},\phi)$ is the confinement coefficient, calculated by the Fourier transform of the spatial function used to confine the phonon wave function inside the particle of diameter ϕ, and $L(\omega,\mathbf{q})$ is the Lorentzian function coming from the oscillating dipole model. For a particle with a diameter ϕ, the possible wave vectors are quantified and given by eq 8:

$$k_n = n\pi/\phi \quad (8)$$

with n being even for the TO phonon mode of Si, $n = 2, 4, ..., n_{max}$, n_{max} being equal to the nearest integer lower or equal to $2\phi/a$, and $a = 0.543$ nm being the Si lattice parameter.

In their model, Faraci et al.[15] choose a sum of sinus cardinal functions to model the confinement effect. This leads to the expression of $C(\mathbf{q},\phi)$ reported in eq 9:

$$C_n(\mathbf{q},\phi) = 3\frac{\sin(q\phi/2)}{\pi^3\phi^3 q(k_n{}^2 - q^2)} \quad (9)$$

The Raman spectrum for a particle of diameter ϕ is then given by eq 10:

$$I_{\text{Raman}}(\omega,\phi) \propto \sum_n \int_{(n\pi-1)/\phi}^{(n\pi+1)/\phi} \frac{C_n{}^2(\mathbf{q},\phi)}{[\omega - \omega'(\mathbf{q})]^2 + (\Gamma/2)^2}\,\mathrm{d}\mathbf{q} \quad (10)$$

with Γ the natural bandwidth, typically fixed to 3 cm^{-1}, and the dispersion curve for the TO phonon modes of silicon taken as that of bulk Si[15] (eq 11):

$$[\omega'(\mathbf{q})]^2 = A + B\cos(a\mathbf{q}/4) \quad (11)$$

In eq 11, $A = 1.714 \times 10^5\ \mathrm{cm}^{-2}$ and $B = 1.00 \times 10^5\ \mathrm{cm}^{-2}$.

The Raman spectrum for a distribution of nc-Si having a diameter ϕ and following the distribution law of eq 4 is then finally given by eq 12:

$$I_{\text{Raman}}(\omega) = \int_{d=0}^{\infty} p(\phi,\phi_0,\sigma)\cdot I(\omega,\phi)\mathrm{d}\phi \quad (12)$$

Comparison with Experimental Data on Multilayered Samples. In Figure 5a are reported both experimental and theoretical photoluminescence spectra of the multilayer sample annealed at 1050 °C. The parameters ΔE, ϕ_0, and σ were fitted to adjust the luminescence model to the experimental emission spectra. Then the values obtained for ϕ_0 and σ were directly used in the phonon confinement model presented above. Therefore it is important to note that no new fitting procedure was applied for the phonon confinement model. Theoretical and experimental Raman spectra are plotted in Figure 5b.

It is clear that the luminescence model enables the photoluminescence spectra to be properly fit. The average fwhm of the photoluminescence emission band of nanocrystals is found at $\Delta E = 35$ meV. This is consistent with the data obtained for isolated silicon quantum dots reported in the article of Sychugov et al.[16] and constitutes another argument in favor of the creation of silicon nanocrystals in the multilayer samples. The photoluminescence spectra represent the sum of emission bands of a macroscopic collection of nanocrystals. The fact that the value of the average fwhm ΔE is consistent with the fwhm value of isolated Si quantum dots in silica pillars[16] is also a hint that the size distribution of nc-Si is rather sharp, which is confirmed by the value of $\sigma = 1.2$ nm found by the fitting procedure. Beyond the good accuracy of the spectrum fitting in Figure 5a, the parameter values are thus fairly self-consistent and justify a posteriori the photoluminescence model we used. But the most interesting result is that the phonon confinement model also gives a good fit of the phonon spectra at around 519 cm^{-1} by using the values of ϕ_0 and σ deduced from luminescence analysis. The two models are thus in close agreement and reveal the useful combination of photoluminescence and Raman spectroscopies to obtain the size distribution of the nc-Si in the sample. It also firmly evidences the better control of electronic and phononic properties of such silicon nanocrystals using multilayered structures. The average size obtained by the spectral fitting procedure is around 5 nm, which is slightly bigger than the thickness of the SiO layer. This could signify that, during the annealing process, the growth of silicon nanocrystals is not strictly confined in the SiO layers. The crystals may also be oblate, with a dimension higher in the plane of the SiO layers. The confinement models (that consider spherical crystals) can account for this geometry by increasing the mean diameter and slightly relaxing the confinement of excitons or phonons.

If we refer to the size distribution of the nc-Si obtained by TEM with a 4-nm SiO layer, the nc-Si diameter is approximately 4.1 ± 1.7 nm.[10] This result is in rather good agreement with the values of ϕ_0 and σ obtained with the theoretical analysis of experimental photoluminescence and Raman spectra (5.13 ± 1.23 nm). The size obtained by spectral fitting is slightly higher than that obtained by TEM. This may be due to the fact that statistics realized with TEM measurement are made by using a rather small number of nc-Si and is very sensitive to the subjective definition of crystalline area by the operator. Moreover, the difference between our model and TEM measurements can also be attributed to residual stress and surface defects of nanocrystals that may exist in such nanometric multilayered structures.[17] Indeed, a compressive residual stress would slightly upshift the Raman phonon peak.[18] While the internal residual stress is not taken into account in our study, the theoretical analysis of spectroscopic results with quantum confinement models and TEM results are in good agreement. This self-consistency constitutes a strong argument in favor of the existence of such confinement effect in nanocrystalline structures.

Conclusion

We studied silicon nanostructures by photoluminescence and Raman spectroscopy. Samples have been made by evaporation and subsequent annealing under vacuum. Two kinds of samples have been elaborated and analyzed. The first kind of sample is, before annealing, constituted by a thick SiO layer. The second one is a SiO/SiO_2 multilayer. The thicknesses of the SiO and SiO_2 layers in the multilayers are of 4 and 5 nm, respectively. In the SiO monolayer sample annealed between 600 and 940 °C, the demixion process induces the appearance of amorphous silicon areas which show a PL band in the visible range and a Raman spectrum with typical large bands at 160 and 490 cm^{-1}. In SiO/SiO_2 multilayer samples annealed at 1050 °C, the diameter of the Si nanocrystals is controlled by the thickness of the SiO layer. The photoluminescence band is intense and rather narrow and the Raman spectrum shows an asymmetric band with a maximum at 519 cm^{-1}. For this sample, the Raman spectrum has been modeled as well as the photoluminescence spectrum. We modified the model of Faraci et al.[15] for Raman spectra and of Meier et al.[13] for photoluminescence spectra by including a size distribution of nc-Si diameters. The corresponding fitted values of central diameter and size distribution width are in good agreement with those measured by TEM. This constitutes good experimental evidence of the confinement effect for both excitons and phonons in silicon nanostructures embedded in silica matrix. Finally, the phenomenological models used in this study enable us to easily and quite confidently retrieve a good estimation of the size distribution of nanocrystals embedded within a dielectric matrix, which is quite interesting from a methodological point of view for quantum dots characterization in such nanostructured systems.

Supporting Information Available: FTIR absorption spectra of the multilayer samples annealed at different temperatures

and HR-TEM image of an isolated silicon nanocrystal in the SiO_2 matrix. This material is available free of charge via the Internet at http://pubs.acs.org.

References and Notes

(1) Canham, L. T. *Appl. Phys. Lett.* **1990**, *57*, 1046–1048.
(2) Linnros, J.; Lalic, N.; Galeckas, A.; Grivickas, V. *J. Appl. Phys.* **1999**, *86*, 6128–6134.
(3) Garrido Fernandez, B.; Lopez, M.; Garcia, C.; Perez-Rodriguez, A.; Morante, J. R.; Bonafos, C.; Carrada, M.; Claverie, A. *J. Appl. Phys.* **2002**, *91*, 798–807.
(4) Shimizu-Iwayama, T.; Kurumado, N.; Hole, D. E.; Townsend, P. D. *J. Appl. Phys.* **1998**, *83*, 6018–6022.
(5) Iacona, F.; Franzo, G.; Spinella, C. *J. Appl. Phys.* **2000**, *87*, 1295–1303.
(6) Ledoux, G.; Guillois, O.; Porterat, D.; Reynaud, C.; Huisken, F.; Kohn, B.; Paillard, V. *Phys. Rev. B* **2000**, *62*, 15942–15951.
(7) Zhang, W. L.; Zhang, S.; Yang, M.; Chen, T. P. *J. Phys. Chem. C* **2010**, *114*, 2414–2420.
(8) Zacharias, M.; Heitmann, J.; Scholz, R.; Kahler, U.; Schmidt, M.; Blasing, J. *Appl. Phys. Lett.* **2002**, *80*, 661–663.
(9) Jambois, O.; Rinnert, H.; Devaux, X.; Vergnat, M. *J. Appl. Phys.* **2006**, *100*, 123504/1–123504/6.
(10) Rinnert, H.; Vergnat, M. *J. Lumin.* **2005**, *113*, 64–68.
(11) Pässler, R. *Solid-State Electron.* **1996**, *39*, 1311–1319.
(12) Kanemitsu, Y.; Uto, H.; Masumoto, Y.; Matsumoto, T.; Futagi, T.; Mimura, H. *Phys. Rev. B* **1993**, *48*, 2827–2830.
(13) Meier, C.; Gondorf, A.; Lüttjohann, S.; Lorke, A.; Wiggers, H. *J. Appl. Phys.* **2007**, *101*, 103112/1–103112/8.
(14) Delerue, C.; Allan, G.; Lannoo, M. *Phys. Rev. B* **1993**, *48*, 11024–11036.
(15) Faraci, G.; Gibilisco, S.; Russo, P.; Pennisi, A. R.; La Rosa, S. *Phys. Rev. B* **2006**, *73*, 033307/1–033307/4.
(16) Sychugov, I.; Juhasz, R.; Valenta, J.; Linnros, J. *Phys. Rev. Lett.* **2005**, *94*, 087405/1–087405/4.
(17) Wellner, A.; Paillard, V.; Bonafos, C.; Coffin, H.; Claverie, A.; Schmidt, B.; Heinig, K. H. *J. Appl. Phys.* **2003**, *94*, 5639–5642.
(18) Arguirov, T.; Mchedlidze, T.; Kittler, M.; Rölver, R.; Berghoff, B.; Först, M.; Spangenberg, B. *Appl. Phys. Lett.* **2006**, *89*, 053111/1–053111/3.

JP1044095